International Journal of Mechanical, Industrial and Aerospace Sciences
ISSN: 2517-9950
Vol:8, No:6, 2014

Packaging in a Multivariate Conceptual Design Synthesis of a BWB Aircraft

Paul Okonkwo , Howard Smith

Abstract—A study to estimate the size of the cabin and major aircraft components as well as detect and avoid interference between internally placed components and the external surface, during the conceptual design synthesis and optimisation to explore the design space of a BWB, was conducted. Sizing of components follows the Bradley cabin sizing and rubber engine scaling procedures to size the cabin and engine respectively. The interference detection and avoidance algorithm relies on the ability of the Class Shape Transform parameterisation technique to generate polynomial functions of the surfaces of a BWB aircraft configuration from the sizes of the cabin and internal objects using few variables. Interference detection is essential in packaging of non-conventional configuration like the BWB because of the non-uniform airfoil-shaped sections and resultant varying internal space. The unique configuration increases the need for a methodology to prevent objects from being placed in locations that do not sufficiently enclose them within the geometry.

Keywords—Packaging, Optimisation, BWB, Parameterisation, Aircraft Conceptual Design.

I. Introduction

THE desire to create environmentally friendly aircraft that are aerodynamically efficient and capable of conveying a large number of passengers over long ranges at reduced direct operating cost led aircraft designers to develop the Blended Wing Body (BWB) aircraft. The BWB represents a paradigm shift in the design of aircraft. It offers immense aerodynamics and environmental benefits and is suitable for the integration of advanced systems and concepts like distributed propulsion systems, jet flaps and laminar flow technology. However, several design challenges have stunted its development into a commercial transport aircraft. Its non-circular fuselage presents a packaging challenge especially in an optimisation routine to explore the design space.

Packaging in aircraft design is provided to size major aircraft components and position them appropriately to obtain a satisfactory static stability margin while avoiding interference of internally placed objects with the external geometry. Packaging implementation consists of sizing, geometry parameterization and interference detection. Sizing models determine the dimensions of major aircraft components while the parameteric model creates the external shape of the aircraft. The sizing and parameterization models are combined in an interference detection algorithm to position the items within the geometry, while ensuring there is sufficient space to accomodate all components. The interference detection also guarantees that positional variations of internal components during optimisation, for instance to obtain good stability margins, do not place objects in an unfeasible space.

Paul Okonkwo is a PhD student at the Department of Aerospace Engineering, Cranfield University, MK430 AL, Bedford, UK(phone: +447774472416; e-mail: pokonkwo1@gmail.com).

Howard Smith is a Professor of Aircraft Design and Head of the Aircraft Design Group, School of Engineering, Department of Aerospace Engineering, Cranfield University, UK(e-mail: howard.smith@cranfield.ac.uk).

The objective of this paper, which is derived from on-going studies on the development of a multivariate design synthesis and optimisation tool to explore the design space of BWB configuration, is to discuss the development of a packaging model to prevent the interference of internal objects with the external surfaces of a BWB aircraft. This paper will cover sizing of major aircraft components, geometry parameterisation using the Class Shape Transformation (CST) parameterisation technique and the application of CST method in interference detection.

II. Sizing

The aircraft components sized in this paper are the cabin, engines, landing gear and baggage compartment. The cabin size is determined from the Kevin Bradley [1] cabin sizing method while the engine(s) is/are rubber-scaled from selected nominal engine to the dimensions required to provide the desired thrust using certain scale factor. Landing gear sizes were developed from the maximum landing weight while the size of baggage compartment is derived from manipulation of the standard dimensions of conventional unit loading devices.

A. Passenger Cabin Sizing

The BWB passenger cabin is sized following the Bradley [1] sizing procedure shown in Fig. 1. Bradley [1] sizing method consists of 3 steps. These are determining the total length of cabin required, the number of bays and dimensioning the cabin.

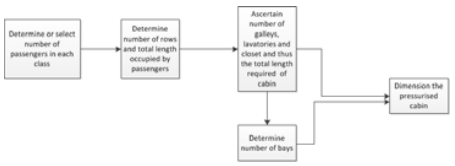

Fig. 1 Procedure for Sizing the Cabin of a BWB

The total length required is determined from (1) by assuming all passengers, lavatories, closets and galleys would be fitted in one long bay. Then choosing a 3×3 , 3×2 and 2×2 seating in tourist, business and first class respectively, in order to maximise the number of passengers with the least

width, and allowing for a wider aisle width than available in current commercial transport, Bradley [1] approximated the width of each bay to be $12ft$.

$$l_{\text{req}} = (n_{\text{Fr}} \cdot p_{\text{F}}) + (n_{\text{Br}} \cdot p_{\text{B}}) + (n_{\text{Tr}} \cdot p_{\text{T}}) + ((n_{\text{gly}} + n_{\text{lav}})36) + (n_{\text{clst}} \cdot 12) \quad (1)$$

l_{req} is length required .
p_{F} is first class seat pitch .
p_{B} is business class seat pitch .
p_{T} is tourist class seat pitch .

Number of seat rows for the different passenger classes, n_{Fr}, n_{Tr} and n_{Br}, is obtained from (2).

$$\begin{aligned} n_{\text{Fr}} &= \frac{n_{\text{Fpax}}}{n_{\text{Fabr}}} \\ n_{\text{Br}} &= \frac{n_{\text{Bpax}}}{n_{\text{Babr}}} \\ n_{\text{Tr}} &= \frac{n_{\text{Tpax}}}{n_{\text{Tabr}}} \end{aligned} \quad (2)$$

n_{Fpax} is the number of first class passengers.
n_{Fabr} is the number seats abreast in the first class.
n_{Bpax} is the number of business class passengers.
n_{Babr} is the number seats abreast in business class.
n_{Tpax} is the number of tourist class passengers.
n_{Tabr} is the number seats abreast in tourist class.

Number of galleys, n_{gly}, is determined from (3):

$$n_{\text{gly}} = 1 + \frac{n_{\text{Fpax}} + n_{\text{Bpax}} + n_{\text{Tpax}}}{100} \quad (3)$$

Number of lavatories, n_{lav}, is derived from (4):

$$n_{\text{lav}} = \left(1 + \frac{n_{\text{Tpax}}}{100}\right) + \left(1 + \frac{n_{\text{Fpax}} + n_{\text{Bpax}}}{60}\right) \quad (4)$$

Number of closets, n_{clst}, is obtained from (5):

$$n_{\text{clst}} = 1 + \frac{n_{\text{Fpax}}}{30} + \frac{n_{\text{Bpax}}}{45} + \frac{n_{\text{Tpax}}}{60} \quad (5)$$

Since, a BWB cabin blends into the outer wing, the root chord of outer wing must be equal to chord of the rib enclosing the passenger compartment. Choosing a thickness to chord ratio of 15% to ensure an acceptable transonic performance, a minimum outer rib chord length of $55ft(16.764m)$ is required to provide sufficient depth to accommodate the upper and lower skin surfaces, passenger decks, internal furnishings and standing height of passenger [1]. Additionally, assuming that the cabin extends from the leading edge to about 70% chord as shown in Fig. 2, a rib chord length of $55ft$ corresponds to a cabin length of $38.5ft$.

Taking the centre-body as a linearly ruled surface, such that for every $6ft$ increase in length, the span increases by $12ft$ or the equivalence of an additional bay as shown in Fig. 3, the maximum length of the outer-wall is set to 44.5ft. Bradley [1] sizing method proposes for lateral expansion of the BWB centrebody in order to maximise the number of passengers that

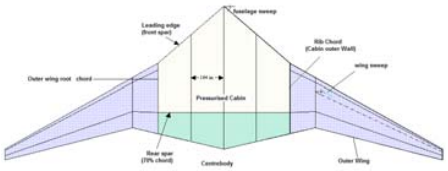

Fig. 2 Planform View of BWB Geometry showing the Parameters used in Cabin Sizing [1]

TABLE I
MaximumUsefulLengthofBays

Number of Bays	Maximum Length (ft)
1	44.5
2	101.3
3	170.4
4	251.8
5	345. 5

could be airlifted with minimal increase in root chord length. Though this lateral expansion could be continued indefinitely, Bradley [1] limits the number of bays to 5.

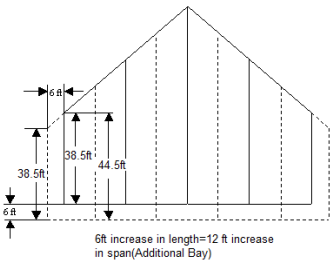

Fig. 3 The BWB Cabin as a Ruled Surface [1]

Substituting, values derived from the foregoing assumptions into (6), the maximum length for any number of bay, n, at a given sweep angle is determined.

$$l_{\text{max}} = nl_{\text{w}} + \frac{w}{2}\tan\Lambda_{\text{fus}} \sum_{i=1}^{n}(i-1) \text{ [1]} \quad (6)$$

i is index or counter,
l_w is the length of outermost wall,
Λ_{fus} is the sweep angle of centrebody leading edge.

Applying (6) to a BWB cabin with a sweep angle of $64°$, the maximum useful length for certain number of bays is obtained and listed in Table I.

Comparing the total length required and the predicted values of maximum useful length for various number of bays given in Table I, the appropriate number of bays is selected. From the number of bays and width of each bay, the width of cabin is calculated by (7) [1].

$$w_{\text{bay}} = w_{\text{ea}} \cdot n_{\text{bay}} \quad (7)$$

w_{bay} is the width of cabin .
w_{ea} is the width of each bay .
n_{bay} is the number of bays.

Having determined the number of bays, the next step in BWB sizing process is to dimension the cabin. This requires determining the lengths of the cabin outermost wall and centreline as well as the lengths of the outer-walls of each bays. The length of the outer-most wall, l_w, of the pressurised cabin, which must be equal or greater than the minimum outer wall chord of 38.5ft, is obtained from (8) by replacing l_{tot} in (6) by l_{req} and solving for l_w [1].

$$l_{\text{w}} = \left(\frac{l_{\text{req}} - \frac{w_{\text{ea}}}{2} \tan \Lambda_{\text{fus}} \sum_{i=1}^{n} (i-1)}{n} \right) \tag{8}$$

The length of BWB cabin centreline is a function of the number of bays, fuselage sweep angle, length of outerwall and the width of each bay and is determined from (9) [1].

$$xl_{\text{p}} = l_{\text{w}} + \frac{w_{\text{ea}}}{2} \tan \Lambda_{\text{fus}} \cdot n_{\text{bay}} \tag{9}$$

The walls of each bay, except the centre bay in a 3-bay arrangement, are usually of different lengths. However, breaking each bay into 2 columns, ensures there are always 2 columns of equal length by symmetry. The columns of equal lengths are recombined into equivalent bays as shown in Fig. 4. The recombination of columns of equal length into equivalent bays ensures the lengths of the outer-board walls of each bay is determined from the lengths of the columns.

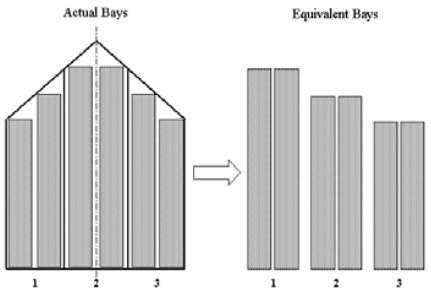

Fig. 4 Converting Seating Areas into Equivalent Bays [1]

Now, assuming the outer walls of the columns in the left picture in Fig. 4, are numbered consecutively from the centreline, $q = 0$ to $q = nfus$ outwards, the length of outer wall of each column, xl_{ea}, is obtained from (10).

$$xl_{\text{ea}} = xl_{\text{p}} - q \left(\frac{w_{\text{ea}}}{2} \cdot \tan \Lambda_{\text{fus}} \right) \tag{10}$$

B. Baggage Compartment Sizing

The size of baggage compartment of a BWB is determined from the number of standard loading devices carried on-board the airplane. The number of unit loading device(ULD) required is obtained from a survey of passenger airplanes of similar range and payload. The study indicates that passenger airplanes generally carry between 10 to 42 ULDs. Opting to use ULD3s with lengths, widths and heights of 1.53m, 2.01m and 1.63m respectively, the lengths of baggage compartments for different quantities and width of baggage compartments as determined from a number of different ULD3s abreast combinations as listed in Table II.

TABLEII
Variation of Length and Width of ULD3s with Number of ULD3s

Length of ULD3(m)	Width of ULD3(m)	Number of ULD3
16.08	6.12	32
18.09	6.12	36
16.08	7.65	40
18.09	7.65	45
12.06	9.18	36
8.04	12.24	32

Now, applying multivariate linear regression to the data shown in Table II, a relationship between length, width of baggage compartment and total number of baggage required is obtained. This relationship is defined in (11). Please note that the width of baggage is derived from the number of containers abreast.

$$l_{\text{bgge}} = \frac{nLD3}{0.3252 w_{\text{bgge}}} \tag{11}$$

l_{bgge} is the length of baggage compartment.
n_{LD3} is the number of ULD3s carried on the airplane.
n_{abr} is the number of ULD3s abreast.
w_{LD3} is the width of each ULD3.
w_{bgge}, the width of the baggage compartment is given by (12):

$$n_{\text{abr}} \cdot w_{\text{LD3}} \tag{12}$$

C. Engine Sizing

Ordinarily, engine sizing would have been irrelevant to packaging and interference detection algorithms because engines are usually externally mounted on the surfaces of conventional configurations. However, the BWB enables engines to be embedded in a boundary layer ingesting, distributed propulsion arrangement. This has made it necessary to size engines to determine the amount of space it requires within the aircraft. Engines are sized using the rubber sizing approach.

Rubber sizing scales a reference engine, by some scaling factor, to dimensions required to provide the desired thrust. Thrust scale factor is the ratio between required thrust and the thrust of the reference engine. For a multi-engined aircraft as is required in distributed propulsion, boundary layer ingestion arrangement, the thrust scale factor is determined from (13).

$$T_{\text{SF}} = \frac{T_{\text{req}}}{n_{\text{eng}} \cdot T_{\text{engRef}}} \tag{13}$$

T_{SF} is the thrust scale factor.

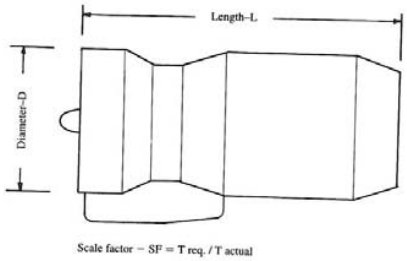

Fig. 5 Rubber Scaling of an Engine [3]

T_{req} is thrust required as determined from selected thrust to weight ratio and estimated maximum take off weight.
n_{eng} is the number of engines.
T_{engRef} is the reference engine thrust.

The dimensions which must be scaled from the selected nominal engine are shown in Fig. 5.

The variation of length, width and weight with the scale factor are obtained for a commercial transport aircraft jet engine from (14), (15) and (16) [3] respectively.

$$l_{\text{eng}} = l_{\text{engRef}} \cdot T_{\text{SF}}^{0.4} \tag{14}$$

l_{eng} is the length of scaled engines.
l_{engRef} is the length of reference engine.

$$D_{\text{eng}} = D_{\text{engRef}} \cdot T_{\text{SF}}^{0.5} \tag{15}$$

D_{eng} is the diameter of scaled engines.
D_{engRef} is the diameter of reference engine.

$$W_{\text{eng}} = W_{\text{engRef}} \cdot T_{\text{SF}}^{1.1} \tag{16}$$

W_{eng} is the weight of scaled engines.
W_{engRef} is the weight of reference engine.

Efficient operation of engines requires the intake inlet to slow down the speed of air entering an engine to about Mach $0.4-0.5$ at the compressor fan face. This is necessary in order to keep the tip speed of compressor blades below the speed of sound with respect to the incoming air [3]. The design parameters required for the design and sizing of the engine intake inlet are defined in Fig. 6.

The length of the engine intake, l_{fb}, is sized according to (17).

$$l_{\text{fb}} = r_{\text{IDl}} \cdot h_{\text{II}} \tag{17}$$

h_{II} is the height of intake inlet.
r_{IDl} is the ratio of intake diameter to length.

Raymer [3] defined the ratio of intake diameter to length, r_{IDl}, by (18).

$$r_{\text{IDl}} = \sqrt{Sr_{\text{Dth}}} \tag{18}$$

The ratio of the areas of inlet diffuser to area of the throat of the engine inlet, Sr_{Dth}, is determined from (19).

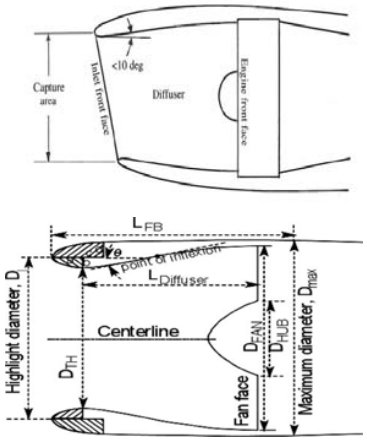

Fig. 6 Definition of Parameters Used in the Design of the Intake Inlet of an Engine [3], [4]

$$Sr_{\text{Dth}} = \frac{Sr_{\text{dff}}}{Sr_{\text{th}}} \tag{19}$$

Sr_{dff} is the area ratio of the inlet diffuser.
Sr_{th} is the area ratio of the throat.

The area ratio of the throat, Sr_{th}, is a function of the cruise Mach number, M_{cr}, as given by (20). The Mach number is however modified by 0.765 to account for the difference in the speed of airflow reaching the engine intake throat from the aircraft cruise Mach Number.

$$Sr_{\text{th}} = \frac{1}{0.765M_{\text{cr}}}\left(\frac{1+0.2(0.765M_{\text{cr}})^2}{1.2}\right)^3 \tag{20}$$

Similarly, the area ratio of the diffuser, Sr_{dfs}, is calculated from (21) with Mach number, M, equal to 0.4, the speed of airflow expected at the compressor fan face.

$$Sr_{\text{dfs}} = \frac{1}{M}\left(\frac{1+0.2M^2}{1.2}\right)^3 \tag{21}$$

The height of the intake inlet, as defined by (22) is a function of the area of the intake at the throat, Si_{th}, and the width of intake inlet, w_{inl}.

$$h_{\text{II}} = \sqrt{\frac{Si_{\text{th}}}{w_{\text{inl}}}} \tag{22}$$

The area of the intake at the throat is obtained from the ratio of the engine demand cross-sectional area and the ratio of the area of the diffuser to throat area [4] as stated in (23).

$$Si_{\text{th}} = \frac{S_{\text{engD}}}{Sr_{\text{Dth}}} \tag{23}$$

Mattingly [5] defined the engine demand cross-sectional area, S_{engD}, by (24). Consequently, with the ratio of the areas of the diffuser to throat already obtained, the area of the intake inlet at the throat is determined.

$$S_{\text{engD}} = \frac{\dot{m}_e}{\rho \cdot v_{\text{inl}}} \tag{24}$$

$\dot{m}$ is the engine air mass flow rate. ρ_{∞} is the freestream air density at the cruise altitude.
$v_{\infty \text{inl}}$ is the freestream inlet speed often taken as a fraction of the cruise Mach No.

The width of the intake inlet, w_{inl}, is a product of the square root of the inlet aspect ratio, A_{inl}, and the area of inlet at he throat as given in (25).

$$w_{\text{inl}} = \sqrt{A_{\text{inl}} \cdot Si_{\text{th}}} \tag{25}$$

Given that the inlet aspect ratio, A_{inl}, ranges from 1-1.2, the width of the inlet could be determined [4].

The length of engine exhaust, l_{ex}, is derived from (26).

$$l_{\text{ex}} = l_{\text{dex}} \cdot \sqrt{T_{\text{SF}}} \tag{26}$$

The exhaust end diameter, D_{exE}, is obtained from (27).

$$D_{\text{exE}} = D_{\text{dex}} \cdot \sqrt{T_{\text{SF}}} \tag{27}$$

D_{dex} is the datum exhaust diameter.

Having determined all necessary parameters, the overall length of the engine bay, l_{eBay}, is derived from (28).

$$l_{\text{eBay}} = l_{\text{eng}} + l_{\text{fb}} + l_{\text{ex}} \tag{28}$$

The width or diameter of the engine bay, w_{eBay}, is obtained from (29).

$$w_{eBay} = (D_{\text{eng}} \cdot n_{\text{eng}}) \tag{29}$$

D. Landing Gear Bay

The landing gear is sized as a function of the maximum landing weight. Maximum landing weight is approximated as 85% of the $MTOW$ [8]. Total length of the landing gear is subsequently determined from (30) [2].

$$lt_{\text{LG}} = \left(\frac{MLW}{k_{\text{LG}}}\right)^{k_{\text{exp}_{\text{LG}}}} \tag{30}$$

MLW is the maximum landing weight.
lt_{LG} is the total length of landing gear.
k_{LG} is constant in correlation to landing gear length.
$k_{\text{exp}_{\text{LG}}}$ is the exponential constant in relation to landing gear length.

Subsequently, the lengths of the nose gear, l_{NG}, is determined from statistically obtained ratio of nose gear to main gear, r_{NG2MG}, as given in (31) .

$$l_{\text{NG}} = \frac{(lt_{\text{LG}} \cdot r_{\text{NG2MG}})}{(r_{\text{NG2MG}} + 2)} \tag{31}$$

While, the length of the main landing gear is determined from (32).

$$l_{\text{MG}} = 0.5 \cdot (lt_{\text{LG}} - l_{\text{NG}}) \tag{32}$$

The diameter and width of main and nose wheel are important parameters in the estimation of the length, height and width of landing gear bays. The diameter of main and nose wheels are estimated by (33) and (34).

$$d_{\text{Mwl}} = f_{\text{Mwl}} \cdot MLW + k_{\text{Mwl}} \tag{33}$$

d_{Mwl} is the diameter of the main wheel.
f_{Mwl} is the factor in correlation to the main wheel.
k_{Mwl} is constant in correlation to the main wheel.

$$d_{\text{Nwl}} = f_{\text{Nwl}} \cdot MLW + k_{\text{Nwl}} \tag{34}$$

d_{Nwl} is the diameter of the nose wheel.
f_{Nwl} is factor in correlation to the nose wheel.
k_{Nwl} is the constant in correlation to the nose wheel.

The width of the nosewheel is taken as $0.432m$ while the width of the mainwheel is determined from (35).

$$w_{\text{Mwl}} = f_{\text{Mwl}} \cdot MLW + k_{\text{wMwl}} \tag{35}$$

w_{Nwl} is the width of the main wheel.
f_{Mwl} is factor in correlation to the main wheel.
k_{wMwl} is the constant in correlation to width of the main wheel.

The lengths of main bay, l_{MBay}, and nose bay, l_{NBay}, are determined from (36) and (37) respectively.

$$l_{\text{MBay}} = 0.5 \cdot d_{\text{Mwl}} + l_{\text{MG}} \tag{36}$$

d_{Mwl} is the diameter of the main wheel.
l_{MG} is the length of the main gear.

$$l_{\text{NBay}} = 0.5 \cdot d_{\text{Nwl}} + l_{\text{NG}} \tag{37}$$

d_{Nwl} is the diameter of the nose wheel.
l_{NG} is the length of the nose gear.

Similarly the width of the main bay, w_{MBay}, and nose bay , w_{NBay}, could be determined by (38) and (39) respectively.

$$w_{MBay} = f_{Mwlwklr} \cdot w_{Mwl} \tag{38}$$

$f_{Mwlwklr}$ is the clearance factor in relation to the main wheel.
w_{Mwl} is the width of the main wheel.

$$w_{NBay} = f_{Nwlwklr} \cdot w_{Nwl} \tag{39}$$

$f_{Nwlwklr}$ is the clearance factor in relation to the nose wheel.

w_{Nwl} is the width of the nose wheel.

The height of the main bay, h_{MBay}, and nose bay, h_{NBay}, are then determined by (40) and (41) respectively.

$$h_{MBay} = f_{Mwldklr} \cdot d_{Mwl} \tag{40}$$

$f_{Mwldklr}$ is the main wheel diameter clearance factor.
d_{Mwl} is the diameter of the main wheel.

$$h_{MBay} = f_{Nwldklr} \cdot d_{Nwl} \tag{41}$$

$f_{Nwldklr}$ is the nose wheel diameter clearance factor.
d_{Nwl} is the diameter of the nose wheel.

III. Arrangement of Major Internal Components within the BWB Geometry

The Blended wing body by virtue of its unique configuration is adaptable to several arrangements of major components. The engine could be podded under the wing like in conventional aircraft, over the wing or aft of the centre-body in a distributed propulsion, boundary layer ingestion arrangement. Similarly, the baggage could be placed under the cabin, beside the outer walls of the cabin or behind the cabin to act as cushion between aft centrebody engines and the passengers. The landing gear are usually positioned in a quadricylce arrangement and retracted into the nose, aircraft under-belly and wings in certain cases while the cabin is often positioned in the centrebody. Some of the common arrangements of major internal components are shown in Fig. 7.

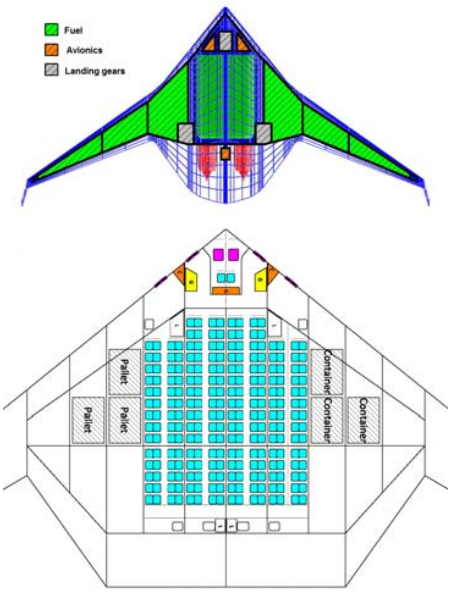

Fig. 7 Common Internal Arrangements of Major Components in a BWB Aircraft [6], [7]

Placing the cabin in the centrebody; engine configured as boundary layer ingesting, embedded, distributed propulsion system aft of the centre-body; and baggage positioned between the engines and the cabin to minimise impact of rotor burst on the passengers and fuel in the outer-wing as shown in Fig. 8, possible span stations for geometry parameterisation are at the centreline, cabin outer wall, root chord and tip chord.

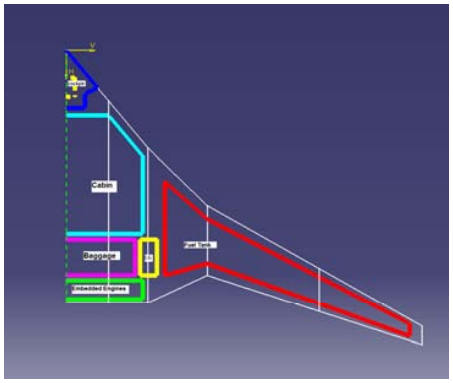

Fig. 8 Implemented Internal Arrangement of Major Components in the Semi-span of a BWB Aircraft

The local chords at the root chord and tip chord stations are the root and tip chords of the aircraft determined from the aircraft taper ratio. The chord at the centreline span position is determined from (42), while the chord at the outer wall of the cabin is obtained from (43).

$$c_{cl} = xl_{cl} + xl_{bgge} + xl_{emb} \tag{42}$$

xl_{cl} is the length of the cabin centreline.
xl_{bgge} is the length of baggage compartment.
xl_{emb} is the length of the portion of engine embedded in the aircraft.

$$c_{owl} = xl_{owl} + xl_{bgge} + xl_{emb} \tag{43}$$

xl_{owl} is the length of the cabin outerwall.

The arrangement of major internal components is essential because it provides the platform for the geometry parameterisation of the aircraft. The positions of the items are used together with their sizes and geometry to determine minimum chords and span stations required for the geometry parameterisation. Additionally, since the interference detection technique implemented in this paper, detects clashes only in the normal or vertical axis, as would be seen later in this paper, the arrangement of items is used with the sizes of the items to set minimum chord and span needed to ensure items are suitably enclosed.

IV. Geometry Parameterisation

Geometry parameterisation provides a mathematical description of an aircraft's geometry. Parameterisation is used in the conceptual design synthesis of the BWB aircraft to generate a polynomial representation of the geometry and hence facilitate easy detection and avoidance of interference between internally placed components and the external geometry. According to Kulfan [9], [10], a

good parameterisation technique must provide smooth and physically realisable shapes using a computationally efficient and numerically stable process that is accurate and consistent. The technique should also be intuitive to permit the manipulation of a geometry using few design variables [9], [10].

Kulfan and Bussoletti [9] reviewed several parameterisation techniques for shape design optimisation including the discrete, polynomial and spline, Bezier curve, orthogonally derived basis function and free-form deformation techniques. The study finds neither of these methods appropriate for a shape design optimisation because they are either computationally expensive or incapable of smoothly modelling complex geometries. Consequently, they developed the Class Shape function Transformation (CST) [9]–[11] technique. The CST parameterisation technique consists of 2 functions; the Class function and the Shape function. The class function defines the general class of geometry while the shape function ensures an analytically well-behaved mathematical function [10].

The Class function is defined by (44):

$$C \begin{matrix} N1 \\ N2 \end{matrix} (\psi) = (\psi)^{N1}(1-\psi)^{N2} \tag{44}$$

$N1 = 0.5$ and $N2 = 1$ for a round nose and aft pointed airfoil.
ψ is the non dimensional airfoil coordinate.
ψ ranges from 0 to 1.

The shape function can be implemented using either the Bernstein polynomial or B-spline functions. Using Bernstein polynomial, the shape function is a product of the summation of unknown coefficients A_i and Bernstein polynomial terms. For a 2-dimensional airfol with upper and lower curves, the shape function for the upper curve, Su_i, is defined by (45).

$$Su_i(\psi) = \sum_{i=1}^{N} Au_i \cdot S_i(\psi) \tag{45}$$

Au_i is the upper curve coefficient.
S_i is the Bernstein polynomial terms given by (46) as:

$$S_i = k_i \psi^i (1-\psi)^{N-i} \tag{46}$$

N is the order of the Bernstein polynomial,
and k_i the binomial coefficient is given by (47).

$$k_i = \frac{N!}{i!(N-i)!} \tag{47}$$

Combining the class and shape function, the equation for the upper curve of a 2-dimensional airfoil is given in (48).

$$\zeta_u(\psi) = C \begin{matrix} N1 \\ N2 \end{matrix} (\psi) Su_i(\psi) + \psi \Delta\zeta_{upper} \tag{48}$$

ζ_{upper}, is the upper curve trailing edge thickness defined by $\frac{\Delta Z u_{TE}}{c}$

The CST for a 3-dimensional wing is derived from the 2-dimensional form by distributing airfoil sections across the wing span [10] and supplementing the class and shape functions for 2D airfoil with twist and local wing shear variables. The parameters used in deriving the CST of a 3D wing are shown in Fig. 9.

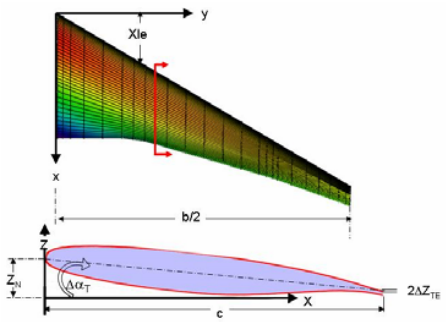

Fig. 9 Parameters used in 3D Wing CST Derivation [10]

The parameters are applied to the design of an arbitrary wing upper surface by (49).

$$\zeta_u(\psi,\eta) = C \begin{matrix} N1 \\ N2 \end{matrix} (\psi) \sum_{i}^{Nx} \sum_{j}^{Ny} [Bu_{i,j} Sy_j(\eta) Sx_i(\psi)] + \psi [\zeta_T(\eta) - \tan\alpha_T(\eta)] + \zeta_N(\eta) \tag{49}$$

The streamwise shape function, $Sx_i(\psi)$ is defined by (50):

$$Sx_i(\psi) = kx_i \psi^i (1-\psi)^{Nx-i} \; for \; i = 0 \; to \; Nx \tag{50}$$

Nx is the order of the Bernstein polynomial in the streamwise direction.
$\alpha_T(\eta)$, is the local wing twist angle.

The streamwise binomial coefficient, kx_i is given by (51):

$$kx_i = \frac{Nx!}{i!(Nx-i)!} \tag{51}$$

The spanwise shape function, $Sy_j(\eta)$ is derived from (52):

$$Sy_j(\eta) = ky_j \eta^j (1-\eta)^{Ny-j} \; for \; j = 0 \; to \; Ny \tag{52}$$

Similarly, the spanwise binomial coefficient, ky_j, is defined by (53):

$$ky_j = \frac{Ny!}{j!(Ny-j)!} \tag{53}$$

$Bu_{i,j}$ is the matrix of upper surface coefficients which are design variables to be determined from optimisation routines.

In a similar vein, the wing lower surface is defined by (54).

$$\zeta_L(\psi,\eta) = C \begin{matrix} N1 \\ N2 \end{matrix} (\psi) \sum_{i}^{Nx} \sum_{j}^{Ny} [Bl_{i,j} Sy_j(\eta) Sx_i(\psi)] + \psi (\zeta_T(\eta) - \tan\alpha_T(\eta)) + \zeta_N(\eta) \tag{54}$$

$Bl_{i,j}$ is the matrix of lower surface coefficients which are design variables determined from optimisation routines.

Wing non-dimensionalised local chord x-coordinate, ψ, which ranges from 0 to 1, is obtained from (55):

$$\psi = \frac{x - x_{LE}(\eta)}{c(\eta)} \tag{55}$$

Non-dimensionalised half span airfoil stations, η, which also ranges from 0 to 1 is obtained from (56):

$$\eta = \frac{2y}{b} \tag{56}$$

$x_{LE}(\eta)$, is the local leading edge coordinate,
and $c(\eta)$, is the local chord length:

Non-dimensional upper surface coordinate, $\zeta_u(\eta)$, is defined in (57):

$$\zeta_u(\eta) = \frac{z_u(\eta)}{c(\eta)} \tag{57}$$

Non-dimensional local wing shear is obtained from (58):

$$\zeta_N(\eta) = \frac{z_N(\eta)}{c(\eta)} \tag{58}$$

To ensure the continuity of surface around the leading edge, Kulfan [10] proposed that $Bl_{0,j} = Bl_{0,j}$.

The physical y, x as well as the upper and lower z-ordinates of the parameterised wing are derived from (59), (60) and (61) respectively.

$$y = \frac{b\eta}{2} \tag{59}$$

$$x = \psi C_{Loc}(\eta) + x_{LE}(\eta) \tag{60}$$

$$\begin{aligned} z_u(x,y) &= \zeta_u(\psi,\eta) C_{Loc}(\eta) \\ z_l(x,y) &= \zeta_l(\psi,\eta) C_{Loc}(\eta) \end{aligned} \tag{61}$$

V. Interference Detection

Intersection detection is necessary in the conceptual design synthesis of unconventional airplane configurations like the BWB because of the non-uniform cross-sectional area variation of the BWB geometry and the need to ensure that internal objects are placed in a feasible location. Additionally, since objects positions could be changed during an optimisation routine, to obtain good static stability margin for instance, there is the need to ensure that objects new locations have sufficient space to enclose the item.

Given that the CST parameterisation technique describes the BWB external geometry by a polynomial function, the interference of internal objects with external geometry is assesed by comparing the physical z-ordinates, $z_i(px_i, py_i)$, of the CST curves obtained from vertices, (px_i, py_i, pz_i), of internal object with the z-ordinate, pz_i, of the object. This is expressed mathematically as :

Given a point vector $P = \begin{pmatrix} p_x \\ p_y \\ p_z \end{pmatrix}$

And a curve represented by a polynomial function:

$$z = f(x, y) \tag{62}$$

Point P is within the boundaries of the geometry described by the the upper and lower curves, z_u and z_l respectively, if (63) and (64) are satisfied:

$$f_u(p_x, p_y) > p_z \tag{63}$$

and

$$f_l(p_x, p_y) < p_z \tag{64}$$

Now assuming internal objects are enclosed in a rectangular bounding box to reduce complexity, interference detection is implemented by first converting physical coordinates, px_i, py_i, of all vertices of any bounding box into ψ, η in order to generate the CST polynomial functions $\zeta_i(\psi, \eta)$ of the upper and lower surfaces required. px_i, py_i is converted into ψ, η by (65) and (66) respectively.

$$\psi_{px_i} = \frac{px_i - \eta_i \tan\Lambda_{LE}(\eta_i)}{c(\eta_i)} \tag{65}$$

$$\eta_{py_i} = \frac{2py_i}{b} \tag{66}$$

With η and ψ computed, $\zeta_i(\psi_{px_i}, \eta_{py_i})$ is determined following (67).

$$\begin{aligned} \zeta_i(\psi_{px_i}, \eta_{py_i}) = C \begin{matrix} N1 \\ N2 \end{matrix} (\psi_{px_i}) \\ \sum_{i}^{Nx} \sum_{j}^{Ny} [Bl_{i,j} Sy_j(\eta_{py_i}) Sx_i(\psi_{px_i})] \\ + \psi_{px_i} (\zeta_T(\eta_{py_i}) - \tan\alpha_T(\eta_{py_i})) + \zeta_N(\eta_{py_i}) \end{aligned} \tag{67}$$

The foregoing is implemented for every vertex within the geometry. Subsequently, the $\zeta_i(\psi_{px_i}, \eta_{py_i})$ representing the wing surfaces at all span stations are converted into the physical z-coordinate, $z_i(px_i, py_i)$, and compared with corresponding objects z-coordinates, pz_i to determine interference. The process of converting to the physical z-ordinates is given by (68).

$$\begin{aligned} z_u(px_i, py_i) &= \zeta_u(\psi_{px_i}, \eta_{py_i}) C_{Loc}(\eta_{py_i}) \\ z_l(px_i, py_i) &= \zeta_l((\psi_{px_i}, \eta_{py_i}) C_{Loc}(\eta py_i) \end{aligned} \tag{68}$$

The object or item tested is considered to be properly enclosed within the aircraft geometry, if $z_u(px_i, py_i)$ and $z_l(px_i, py_i)$ obtained from all vertices of the object satisfy (69).

$$z_u(px_i, py_i) > pz_i z_l(px_i, py_i) < pz_i \tag{69}$$

It is imperative to note that the interference detection just described in this paper detects only internal object's violation of vertical or normal axis $z - axis$ boundaries of the geometry. Longitudinal(streamwise) and lateral(spanwise) interference detection is done using the chords and span of the airplane respectively. Additionally, since it would be computationally expensive to parametrically define all curves at every possible span station on the wing, intersection of objects lying between 2 span stations are determined by interpolating the curves bounding the affected span station. Notwithstanding, in order to improve accuracy, it is essential for the greatest distance between parameterised span stations to be less than the least width of internal objects within the geometry. In this way only one side of any object can lie between 2 span stations at any time rather than the complete object.

Interpolation between 2 span stations is implemented by feeding the x-components of objects and bounding adjacent span stations to determine $z_i(px^*, py_i)$ and $z_{i+1}(px^*, py_{i+1})$ of the upper and lower surface. Applying the linear interpolation theorem stated in (70), the z^* is determined. The z^* obtained is then compared with pz^* to determine if object interferes with geometry or is well enclosed.

$$z^* = z_i + \frac{(z_{i+1} - z_i)(y^* - y_i)}{y_{i+1} - y_i} \tag{70}$$

Knowing that a CST parameterisation is given in terms of ψ and η, the physical coordinates or vertices of internal objects is converted to the form required for CST parameterisation by first converting py_i and px_i into η and ψ respectively using (71) and (72) respectively.

$$\eta = \frac{2py_i}{b} \tag{71}$$

$$\psi = \frac{px_i - x_{LE}(\eta)}{c_{Local}(\eta)} \tag{72}$$

The local leading edge x-coordinate is a function of the sweep angle and obtained as:

$x_{LE}(\eta) = \eta \times \tan \Lambda_{LE}$
b is the wing span.

The η and ψ obtained are subsequently substituted into (73) and (74) to determine the physical upper and lower surface z-coordinates, $zu_i(x_i, y_i)$ and $zl_i(x_i, y_i)$, respectively required for interference detection.

$$z_u(x, y) = \zeta_u(\psi, \eta) C_{Local}(\eta) \tag{73}$$

$$z_l(x, y) = \zeta_L(\psi, \eta) C_{Local}(\eta) \tag{74}$$

VI. Conclusion

Packaging is an essential module in the conceptual design synthesis of the BWB because of the non uniform cross-section of the aircraft's geometry. This paper describes several sizing models used to dimension major internal components of a BWB aircraft during a conceptual design synthesis as well as provide a means to detect interference of internal objects with the external geometry.

The interference detection methodology detects when internal objects clashes with external shape using the polynomial characteristics of the parametric model provided by CST parameterisation technique. The CST parameterisation technique is also able to represent a BWB geometry with very few design variables making it suitable for shape design optimisation.

A major limitation of interference detection using the CST parameterisation approach is that it has to be repeated for all objects vertices within the geometry. There is therefore the need for further work to determine how to improve the efficiency of the process. Nevertheless, interference detection capbility in a conceptual design synthesis of the BWB will reduce several man-hour loss, during preliminary design, resulting from packaging difficulties.

Acknowledgment

The authors acknowledge the support of the Department of Aerospace Engineering, Cranfield University, UK as well as the Petroleum Technology Development Fund, Nigeria for this study.

References

[1] Bradley, KR, A Sizing Methodology for the Conceptual Design of Blended-Wing-Body Transports,NASA CR, 2004.
[2] Niyomthai, N, Packaging and Configuration Design Aspect of UCAV Concept Synthesis and Optimisation, Ph.D Thesis, School of Engineering, Cranfield University, 2002.
[3] Raymer, DP, Aircraft Design: A Conceptual Approach, Fourth Edition,AIAA Education Series, Blacksburg, Virginia, Schetz, JA, 2006.
[4] Kundu, AK, Aircraft Design, Cambridge University Press, New York,Edited by Wei Shyy and Michael J. Rycroft, 2010.
[5] Mattingly, JD, Heiser,WH and Pratt,TD, Aircraft Engine Design, American Institute of Aeronautics and Astronautics, Inc. 1801 Alexander Bell Drive, Reston, VA 20191-4344, Edited by J. S. Przemieniecki, 2002.
[6] Nickol, CL, McCullers, LA, Hybrid Wing Body Configuration System Studies, 47th AIAA-2009-931, AIAA Aerospace Sciences Meeting, 5-8 January 2009.
[7] Zhou, W, Cabin Environment and Air Quality in Civil Transport Aircraft, MSc Research Thesis, School of Engineering, Cranfield University, 2011.
[8] Howe,D, Aircraft Conceptual Design Synthesis, Professional Engineering Publishing Limited, London and Bury, ST Edmunds, UK,2000
[9] Kulfan, MB and Bussoletti, JE, Fundamental Parametric Geometry Representations for Aircraft Component Shape, 11th AIAA/ISSMO Multidisciplinary Analysis and Optimization Conference:The Modeling and Simulation Frontier for Multidisciplinary Design Optimization, 2006.
[10] Kulfan, MB, Universal Parametric Geometry Representation Method,Journal of Aircraft,Vol.45, 2008.
[11] Kulfan, MB, CST Universal Parametric Geometry Representation Method With Applications to Supersonic Aircraft, Fourth International Conference on Flow Dynamics Sendai International Center Sendai, Japan, 2007.

Paul Okonkwo is currently in the final year of his Ph.D study at Cranfield University, School of Engineering. He obtained Msc Aerospace Engineering (Aircraft Design) from the Delft University of Technology, the Netherlands in 2009. His interests are aircraft design and multidisciplinary optimisation.

Howard Smith is a Professor of Aircraft Design. He is the head of the Aerospace Design Centre at Cranfield University and has led a number of Aircraft Conceptual Design research projects around the world.